Spatial Point Processes and Temporal Inferences Using Moran Statistics

Jennifer L. Matthews* Norou Diawara † Rachel Johnson ‡

Abstract

Spatial autocorrelation is captured using Moran's index. The later quantifies the degree of dispersion (or spread) of events or objects in space. When investigating data in an area, a single Moran statistic may not give a sufficient summary of the autocorrelation spread. However, by partitioning the area and taking the Moran statistics of the subareas, patterns of the local neighbors not otherwise apparent are discovered. We consider the model of the spread of an infectious disease, incorporate time factor, and simulate a multilevel Poisson process where the dependence among the levels is captured by the rate of increase of the disease spread over time, steered by a common factor in the scale. The main consequence of our results is that our Moran statistic is calculated from an explicit algorithm in a Monte Carlo simulation setting. Results are compared to Geary's statistics and estimates of parameters under Poisson process are given.

Key Words: spatial statistics, temporal, autocorrelation, Moran statistics, Palm distribution

1. Introduction

Spatial structure is an important interface in describing the evolution and progress of many events, such as disease progression in space and time. The data to analyze then capture the variations and causality of the underlying process of the events. As described in design of experiments, the ideas of variation and causality can be linked to the blocking, randomization, replication and resampling. The density of the spread follows various sampling and spatial kriging methods. These concepts are also found in earlier literature as shown in Figure **??** of the Spanish conquest in the early 1500's of the current day Guatemala. The map shows the progression of the conquest in space and time.

As a process, the models that have been proposed may not detect the subtle changes over space and time. The Moran statistic provides a sufficient summary of the degree of dispersion (or spread) of events in space. We suggest time-dependent Moran statistics. However, by segmenting the total area into clusters, the space is then a random field, where each point or occurrence becomes an event of interest for the next time point. The process is captured as a conditional probability model, and the statistics of interests are computed locally. Simulated and real data examples are performed to validate clustering techniques.

The manuscript is organized as follows. Section 2 presents a review of spatial models. Section 3 generalizes the model of dependent Palm distribution with a temporal component. Inferences are investigated in Section 4 with Moran statistics. Simulation and real data examples are analyzed in Section 5, and a summary is provided in Section 6.

*Department of Mathematics, U.S. Naval Academy, Annapolis, MD 21402, USA; E-mail: jmatthew@usna.edu

†Department of Mathematics and Statistics, Old Dominion University, Norfolk, VA 23529, USA; E-mail: ndiawara@odu.edu

‡Department of Communication Disorders and Special Education,Old Dominion University, Norfolk, VA 23529, USA; E-mail: r1johnson@odu.edu

Figure 1. Spatio-temporal map of Spanish conquest.

Figure 2. Spatial point processes.

2. Spatial Models

A point process is a random field where each point represents an event of interest. Point processes have been used to describe events in many fields such as in life testing and epidemiology (disease cases), astronomy (patterns of stars) and described in Cliff and Ord (1981), Coeurjolly et al. (2016, 2017) and in Baddeley et al. (2016). Referring to the area where the spread will be noticeable, the event depends on the knowledge during presampling, adequate description in space and time. The factors that make the prediction challenging are due to the heterogeneity in the terrain in space and time. By using natural embedding so that compactness is preserved (Kallenberg, year) and knowledge from time consecutive observations, we are building a better clustering, and the measure of spatio-temporal pattern is validated via the Moran statistics.

In a one-dimensional setting, these events are described as arrival of customers in a queue, adding time to it. In two-dimensional system, the events can be described in terms of latitude and longitude, showing the terrain characteristics, over time.

Conny Palm, a Swedish telegraphist, applied the stochastic process to telephone exchanges in 1943. He used a Poisson distribution function for the number of incoming calls to an exchange in a given period of time, in studying the properties point process. By adding conditional probabilities, he formulated the now call Palm distribution. We apply such an idea to the finite dimensional sequence of distributions

Considering the area as a measurable spaces with an associated σ-field denoted as $\mathcal{T}$, we associate a random measure ψ that can be described as the count of occurrences of events of interest. In a simple setting, the space can be thought as a real line or a Borel set, with the Poisson count as process. For any location, denoted as s, the count generated as that location with respect to the σ-field,

Palm distribution at location s of an event of interest is defined as:

(2.1)

where ξ is a random measure, with associated finite mean measure μ.

The reduced Palm distribution of the point process at location s is described as the point process generated at s, after its elimination. It is described as Q_s and defined as $Q_s = P_s \circ (\mu - \delta_s)^{-1}$, where $\xi(s) > 0$. Under the reduced Palm Q_s, the process behaves as a superimposed birth process with parents removed and the count is a weighted part of the space.

3. Spatio-temporal Models

The formulation of the model is based on the spread to the incremental time and area susceptible. As shown in Stoyan et al. (1995), the expected process extends to a nested process in time, and is expressed as:

(3.1)

where h is any function of the point process $\underset{\sim}{x}$, with associated density function f and q_t is the number of subareas at time t. To keep the model tractable, the sequence of σ-fields are kept time-dependent by nesting them within the previous time σ-fields and all exchangeable processes capture the probabilistic justification for resolutions with $q_{t-1} \leq q_t$.

Under the proposed Palm distribution, for a set $B^t_{k(t)}$ at time t, $1 \leq k(t) \leq q_t$, the Palm process is then expressed as:

$$P_{t,s}(B^t_{k(t)}) = \frac{\mathbb{E}[\xi_t(ds); \gamma_t \in B^t_{k(t)}]}{\mathbb{E}[\xi_t(ds)]},\ s \in B^t_{k(t)},\ B^t_{k(t)} \in \mathcal{T},$$

where ξ_t is a random measure. The reduced Palm distribution is then $Q_{t,s} = P_{t,s} \circ (\mu - \delta_s)^{-1}$.

4. Statistical Inference

Estimation is still of great interest as expressed in Datta et al. (2016), who suggested a nearest neighbor Gaussian process technique with concern when locations have large groups. The likelihood form we will consider here is expressed as the dependence of different parameters in space and time. Some of the challenges for the model formulation are overcome by: allowing flexible area sizes, applying isotropic properties of the processes, and nesting the areas consecutively in time. Our approach avoids the use of large rank matrices to invert, and rather introduces the random field to a finer dimensional conditionally spaced distribution. For the time series data (Vaillant et al., 2011) and a partitioned time interval with pairs of observations $(t_{i-1}, t_i),\ i = 1, \ldots, m$, the Moran statistic based on a nearest neighbor scheme is defined as:

$$M_i = \sum_{(x,y) \in B} w_{(x,y)} \mathbf{1}_{[0,t_{i-1}]}(T_x) \mathbf{1}_{(t_{i-1},t_i]}(T_y),$$

with $w_{(x,y)}$ a weight between neighbors.

The proposed space-time Moran statistic is defined as:

$$M^t_k = \sum_{u,u' \in B^t_{k(t)}} w_{u,u'} \mathbf{1}_{[t-1,t)}(T_u, T_{u'}),\ \ k \geq 1,\ \ t \geq 1,$$

where $B^t_{k(t)}$ defines the processes subareas, and nesting the areas consecutively in time. The chosen weight is a function of the nearest neighbor Gaussian process, and offers full spatial model at each time period.

The likelihood of the observed process is time and space dependent. If the total area at time t is partitioned into q_t subareas as $B_1, \ldots, B_{q_t}$, with the number of occurring events as $n_1, \ldots, n_{q_t}$, then the model counts can be described as:

$$x_{k(t)} = g(B_{k_t}^t) + \varepsilon_{k(t)}, \quad 1 \leq k(t) \leq q_t,$$

where g is a function of the spread/propagation subarea $B_{k(t)}$ and $\varepsilon_{k(t)}$ is the spread/propagation reconstruction error vector. Under **span** cluster detection,

$$\begin{aligned} \varepsilon_{k(t)} &= (\varepsilon_{1_{k(t)}}, \varepsilon_{2_{k(t)}}, \ldots \varepsilon_{n_{k(t)}}), \quad \text{is such that} \\ f(\varepsilon_{j_{k(t)}}) &= e^{-\alpha_{k(t)} + \beta_{k(t)} h(\varepsilon_{j_{k(t)}})}, \quad 1 \leq j \leq n_{k(t)} \end{aligned}$$

as in Wen and Kedem (2009) and Walther (2009), where h is the tilt function and $\alpha_{k(t)}$ and $\beta_{k(t)}$ are scalars depending on h.

The spatial process is guided by the process between observations of the underlying random field. Our intended contribution is to build a fully (Markovian) parameter estimation and kriging on the residual processes. Turning to predictions, the likelihood function of the errors is:

$$L_t(\alpha_t, \beta_t) = \prod_{k_t=1}^{q_t} \prod_{j=1}^{n_{k(t)}} f(\varepsilon_{j_{k(t)}}) \times p_{t,s},$$

and under the reduced palm distribution:

$$L_t(\alpha_t, \beta_t) = \prod_{k_t=1}^{q_t} \prod_{j=1}^{n_{k(t)}} e^{-\alpha_{k_t} + \beta_{k_t} h(\varepsilon_{j_{k_t}})} \times Q_{t, s_{k(t-1)}}(\varepsilon_{j_{k_t}}).$$

The computational benefits gained from the simplication in the likelihood form are described in the next section.

5. Simulation and Data Examples

5.1. Simulation Example

The model is implemented as a series of time dependent routines. In the simulation setting, we start with a random number of points at time $t = 1$ that are followed over four consecutive time points. Figure 3 displays the number of points generated at time $t = 2$, and the subsequent points generated at time $t = 3$ within one of the selected subareas called disk 1 in shown in Figure 4. The points are generated under a conditional Poisson model with mean parameter $\lambda = 2$, from one time to the next. For locally dependent processes, and dependent superposition of point processes, the Poisson process is an approximation from the point of view of the death process and Palm theory as presented in Chen and Xia (2011). The output in Table 5.1 shows that at time $t = 3$, disk 3 did not generate enough points to have a computable Moran statistic.

Following each of the subareas, clustering within some of the subareas becomes noticeable (see Figure 5), in conformity with the size of the subarea and the parameters associated with the Palm parameters. Computing alongside the associated Moran's values, the later also captures the measure of spatial dependence within each of the subareas. Comparing the global Moran with the local ones at each time points, an oversimplification is avoided, and cluster effects are discovered in the presence of the spatial dependence.

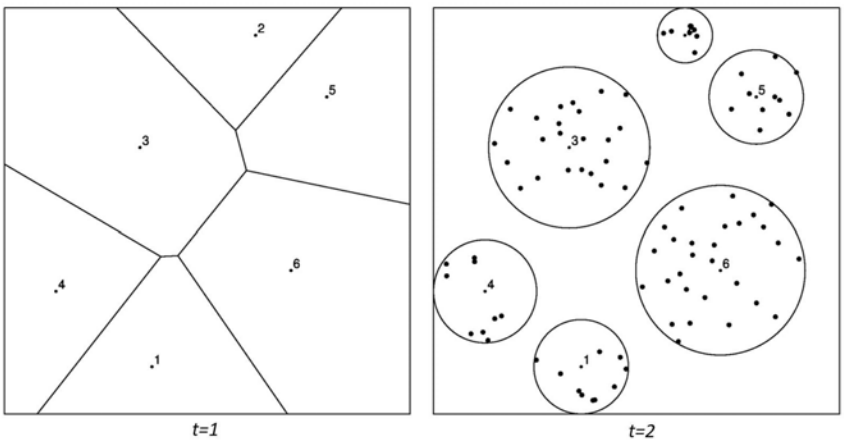

Figure 3. Simulation example at $t = 1$ and $t = 2$.

Table 1. Moran and Geary Values for time $t = 2$

Disk	Points	Area	Moran's	Geary's C
1	10	1.064	158.18	2.444
2	7	0.361	129.29	1.998
3	24	3.096	453.09	7.000
4	9	1.266	111.58	1.724
5	10	1.058	116.03	1.793
6	28	3.415	542.49	8.382

5.2. Real Data Example

The proposed approach is applied to brain image data. For the spatial model, we first focus on the absolute values of the hemoglobin oxygenation (HbO), deoxygenation (HbR) and total (HbT) intensity signals observed in three regions, optodes 1, 2 and 15, in the prefrontal cortex (PFC) during speech for two participants with chronic acquired apraxia of speech and aphasia who participated in a speech motor learning intervention. We focus on three stages of the intervention over 12 days. The brain is depicted as a space with optodes as locations (see Figure 6) and the distances are calculated between optodes with the distance between i and i taken from a central node along the brain stem.

The spatio-temporal Moran statistics are defined as:

$$M_{i,j}^{t} = \sum_{i,j} w_{ij} f(p_i, p_j) = \sum_{i,j} \exp^{-d_{ij}/\bar{d}} |o_i - o_j|,$$

where o_i and o_j are the observed values at optodes i and j for time t.

Calculating distances as described above results in the following distance matrix:

$$d_{ij} = \begin{bmatrix} 4 & 1 & 7 \\ 1 & 4 & 8 \\ 7 & 8 & 4 \end{bmatrix}.$$

Next, we calculate the geographical weights defined as $w_{ij} = e^{-d_{ij}/\bar{d}}$, where $\bar{d}$ is

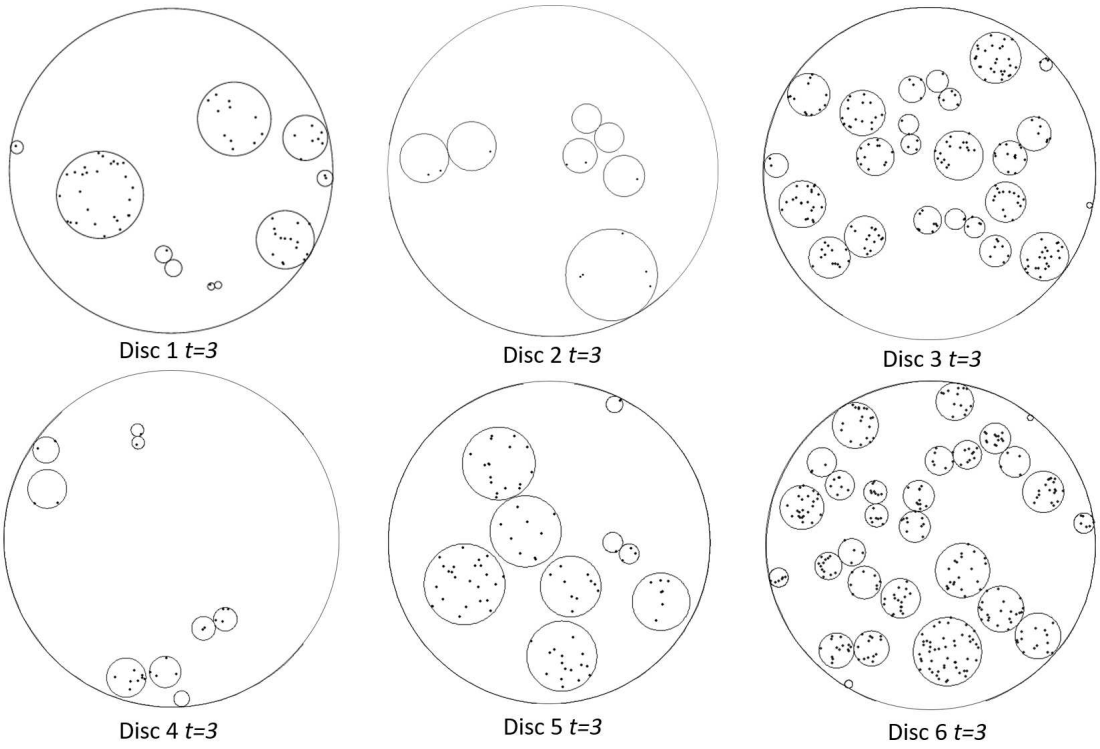

Figure 4. Disk 1 subareas at $t = 3$.

Table 2. Non-zero Moran and Geary Values for Disk 1 at time $t = 3$

Disk	Points	Area	Moran's	Geary's C
1	28	1.905	779.89	5.101
5	11	1.362	125.23	0.819
8	2	0.065	20.11	0.132
9	15	1.183	337.63	2.208
10	7	0.508	80.63	0.527

the average of distances between all possible pairs of points i and j:

$$w_{ij} = \begin{bmatrix} 0.2765 & 0.7251 & 0.01054 \\ 0.7251 & 0.2765 & 0.0764 \\ 0.1054 & 0.0764 & 0.2765 \end{bmatrix}.$$

Then we calculate the Moran statistics for each participant at each stage. Figure 7 shows the graphs of the Moran statistics; a Loess smoothing curve has been added to easily detect trends between participants.

The degree of correlation measured here by the Moran statistics between the participants indicates that the correlation between optodes 1 and 2 (BA 46) vs optode 15 (BA 9) is always higher for Participant 1 (red) in stage 1, whereas in stages 2 and 3, the correlations cross. This last remark is especially visible in stage 2 after day 6. This shows that there is a magnitude of PFC activity (HbO, HbR, and HbT) represented in stage 1 that lessens in stage 2 and 3 over time. This indicates that for Participant 1, the cognitive control processes to maintain the rules to respond and the need to inhibit previously learned behavior decrease with practice. There is a

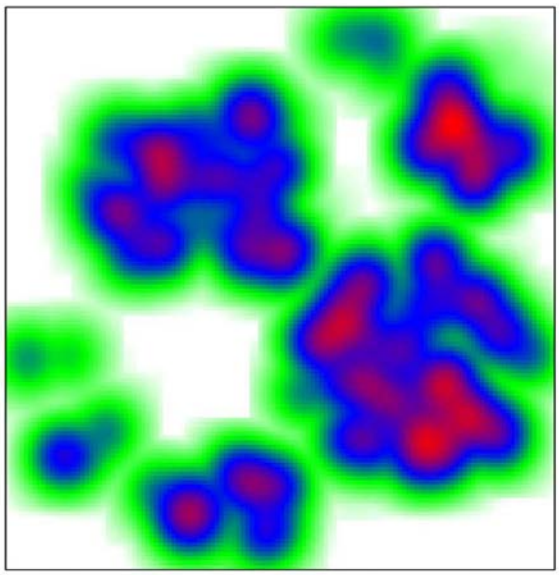

Figure 5. Apparent spatial clustering through $t = 5$.

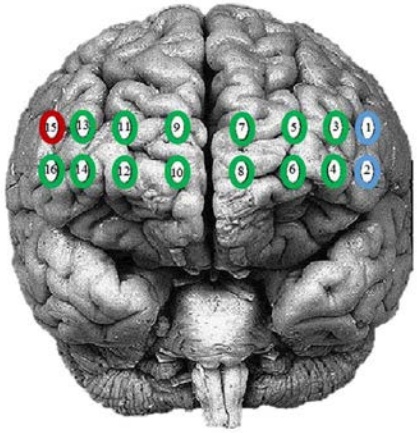

Figure 6. Prefrontal cortex optodes depiction.

decrease in the cognitive effort similar to the tasks completed following a model as in stage 1 (see Glascher et al., 2012). Indeed, there are signs that BA 46 (optodes 1 and 2) activity changed based on the stage of practice across days. Under HbO, oxygenation increases mainly in stage 1, suggesting that Participant 1 had a higher level of activity than Participant 2. From the Moran statistics it appears that over time the activity effect will stabilize and merge with practice.

6. Conclusion

We have proposed a tractable time-dependent model for spatial point processes and developed a subarea based spatial estimation analysis. Challenges faced in the formulation and computational burden are overcome by selecting the Palm distribution and revising the algorithm where resolution is scaled at each time point. The stratification and clustering of events of interest are captured by the Moran statistics over time. Results in the simulations and application to real data show that the likelihood method considered yield better estimation , and is able to incorporate the natural

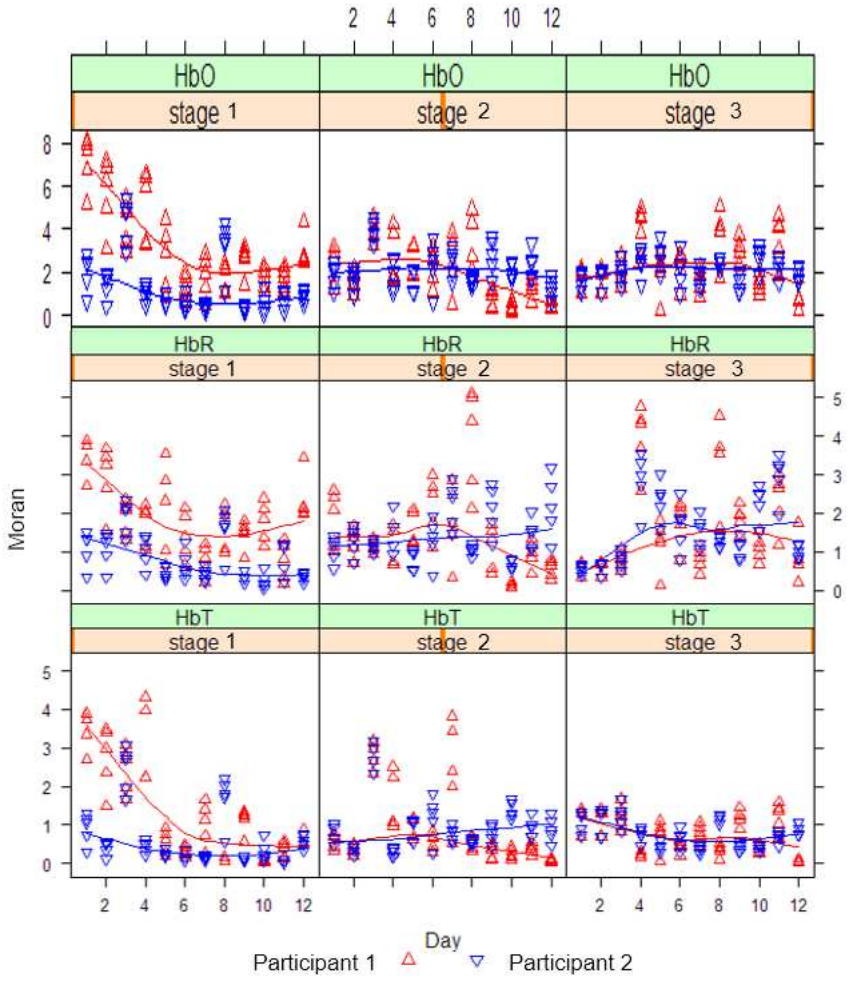

Figure 7. HbO, HbR, and HbT Moran statistics for Participant 1 and Participant 2 through 12 days of intervention.

design mechanism. Patterns and clusters that are time sensitive are then discovered. Even with the introduction of covariates, the model shows higher performance than the naive analysis method.

Extension of the models are under study in the context of Palm measures and subject specific information. Besides challenges due to the large data set or high dimensionality, the concepts of sensitivity, specificity and misclassification for the subject in the location are examined as they depend on the corresponding covariate-adjusted information.

REFERENCES

Anselin, L. (1995), "Local Indicators of Spatial Association - LISA, *Geographical Analysis*, Vol. 27(2), pp. 93–115.

Baddeley, A., Rubak, E., and Turner, R. (2016), *Spatial Point Patterns: Methodology and Applications with R*, CRC Press.

Bui, N., Lorio, J., Diawara, N., Das, K., and Waller, L. (2018), "New Approaches to Model Simulated Spatio-Temporal Moran's Index, *Journal of Probability and Statistical Science*, Vol. 16 (1), pp. 11–24.

Chen, L. H. Y., Xia, A (2011), "Poisson Process Approximation for Dependent Superposition of Point Processes," *Bernoulli*, 17(2), pp. 530–544.

Cliff, A.D. and Ord, J.K. (1981), *Spatial Processes: Models and Applications*, London, Pion.

Cressie, N. and Wikle, C.K. (2011), *Statistics for Spatio-Temporal Data*, Wiley.

Coeurjolly, J., Møller, J., & Waagapeterson, R. (2016), "A Tutorial on Palm Distributions for Spatial Point Processes," *International Statistical Review*, 0, 0, 1–17.

Coeurjolly, J. F., Møller, J., & Waagepetersen, R. (2017), "Palm Distributions for Log Gaussian Cox Processes," *Scandinavian Journal of Statistics*, 44, pp. 192–203.

Datta, A., Banerjee, S., Finley, A. O., and Gelfand, A. E. (2016), "Hierarchical Nearest-Neighbor Gaussian Process Models for Large Geostatistical Datasets," *Journal of the American Statistical Association*, 111, pp. 800–812.

Glascher, J., Adolphs, R., Damasio, H., et al. "Lesion Mapping of Cognitive Control and Value-based Decision Making in the Prefrontal Cortex," it Proceeding of the National Academy of Science USA, 2012, 109(36), pp. 14681–14686.

Kallenberg, O. (2002), *Foundations of Modern Probability* (Second Edition), New York: Springer.

Lorio, J., Diawara, N. and Waller, L. (2018), "Density estimation of spatio-temporal point patterns using Moran's statistics, *International Journal of Statistics and Probability*, Vol. 7 (2), pp. 80–90. DOI: 10.5539/ijsp.v7n2p80

Moran, P.A.P. (1950), "Notes on Continuous Stochastic Phenomena, *Biometrika*, Vol. 37, No. 1–2, pp. 17–23

Martin, R.L. and Oeppen, J.E. (1975), "The identification of regional forecasting models using space-time correlation functions," *Transactions of the Institute of British Geographers*, 66, pp. 95–118. DOI: 10.2307/621623

Möller, J., and Diáz-Avalos (2010), "Structured Spatio-Temporal Shot-Noise Cox Point Process Models, with a View to Modelling Forest Fires," *Scandinavian Journal of Statistics*, Vol. 37(1), pp. 2–25.

Resnick, S.I. (2002), *Adventures in Stochastic Processes*, Birkh. . . auser, Boston.

Stoyan, D., Kendall, W. S.,and Mecke, J. (1995), *Stochastic Geometry and its Applications* (Second Edition), Wiley.

Vaillant, J., Puggioni, G., Waller, L.A. and Daugrois, J. (2011), "A spatio-temporal analysis of the spread of sugarcane yellow leaf virus, *Journal of Time Series Analysis*, Vol. 32, pp. 392–406.

Walther, G. (2009), "Inference and Modeling with Log-concave Distributions," *Statistical Science*, 24(3), pp. 319–327.

Wen, S. and Kedem, B. (2009), "A Semiparametric Cluster Detection Method - a Comprehensive Power Comparison with Kulldorf's Method," *International Journal of Health Geographics*, 8, 73–89.